

Analysis of a mathematical model for malaria using data-driven approach

Adithya Rajnarayanan¹, Manoj Kumar^{1,*}

¹School of Engineering and Science

Indian Institute of Technology Madras, Zanzibar
Tanzania

*Corresponding author's email: manoj@iitmz.ac.in

Abstract: Malaria is one of the deadliest diseases in the world, every year millions of people become victims of this disease and many even lose their lives. Medical professionals and the government could take accurate measures to protect the people only when the disease dynamics are understood clearly. In this work, we propose a compartmental model to study the dynamics of malaria. We consider the transmission rate dependent on temperature and altitude. We performed the steady state analysis on the proposed model and checked the stability of the disease-free and endemic steady state. An artificial neural network (ANN) is applied to the formulated model to predict the trajectory of all five compartments following the mathematical analysis. Three different neural network architectures namely Artificial neural network (ANN), convolution neural network (CNN), and Recurrent neural network (RNN) are used to estimate these parameters from the trajectory of the data. To understand the severity of a disease, it is essential to calculate the risk associated with the disease. In this work, the risk is calculated using dynamic mode decomposition(DMD) from the trajectory of the infected people.

Key Words: Malaria model, Compartmental model, Data-driven methods, Neural network, DMD.

AMS Subject Classification: 92B05, 92B20, 92D25, 92D30 ¹

1 Introduction

According to the WHO report in the year 2022; of all the nations Africa bore the maximum malaria burden. Of all the cases in the world, 94 % of the cases are from Africa, which consists of 233 million cases, and 95 % of total global deaths which consist of 58000 deaths (see Figure 1). It can be clearly understood from the statistics that malaria can cause a huge amount of death in the African continent and it is therefore essential to develop a model which can help doctors and health professionals to understand the disease dynamics in a much better way.

Differential equations-based compartmental models are generally used to analyze the disease transmission. In this method, the entire population is divided into non-overlapping sequential compartments, and the flow of people from one compartment to another is studied using ordinary differential equations. Some of the most commonly used compartments are SIR(susceptible, infected, recovered), SIRD (susceptible infected, recovered, death), and SIRDV(susceptible, infected, recovered, death, vaccinated). Out of all these the

¹*Corresponding author's email

simplest and most used model is the SIR model. Analyzing a population using compartmental models has a lot of advantages, which include reducing the complexity of disease transmission, and providing a framework for predicting future states, these models are extremely flexible and can adapt extra compartments in the future if there is a requirement, compartmental models provide a clear visualization of the system’s dynamics.

One of the earliest models for malaria analysis was built by Ross and it consists of only two compartments one for infected humans and the other one for infected mosquitoes, the parameters that were incorporated were biting rate, recovery rate, and death rate. One of the main limitations of this model is that the parasite’s latent period was not considered which is one of the most important factors for malaria transmission. To understand more about this, model one may refer to [1–4]. After the Ross model, MacDonald developed the next model, which consists of three compartments with both susceptible and infected compartments for mosquitoes and only the infected compartment for human beings. In this model, even though the latent period of parasites in the mosquito was considered, however, the latent period of parasites inside humans was not considered which became a major limitation of this model, to understand more about this model one may refer [5]. Finally, we have the Anderson model which has four compartments where for both the species the susceptible and infected compartments were considered, to know more about this model one may read [6]. To know more about mathematical models of malaria one may refer to the review article [7].

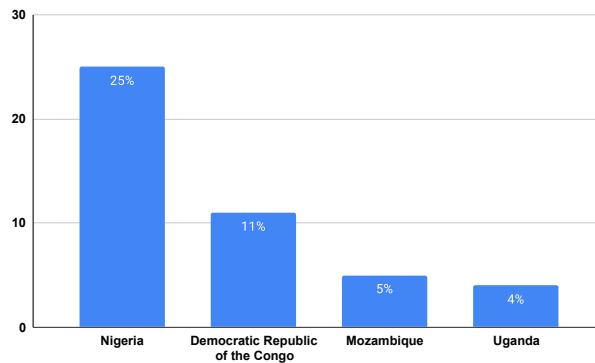


Figure 1: In 2017, four countries from Africa accounted for 45% of all malaria cases worldwide.

In Ogueda et al. [8], a variant of PINN (physics-informed neural network) called DINN (disease-informed neural network) has been used as a deep learning model. The compartmental model SIRD was used to understand the dynamics of the model, where the dynamics of people traveling from one city to another were also considered. The main aim of this work was to predict various parameters, such as rate of transmission, mortality, and recovery, for the cities taken into consideration, along with the rate of movement of people between the cities. In Schiassi et al. [9], the theory of physics-informed learning was combined with the theory of functional connections. For three different compartmental models namely SIR, SIER, and SIERS the transmission rate, recovery rate, and reproduction number were predicted. In Ning et al. [10] using PINN and SEIRD compartmental model a one-week trajectory was calculated using the COVID-19 data for Italy and along with that, the parameters such as transmission rate, recovery rate, and death rate were predicted from 20 Feb to 25 June. In Ning et al. [11] a variant of the PINN called Euler iteration augmented physics informed neural networks was implemented along with the SIRD compartment model to predict the various transmission rates such as transmission rate, death rate, and along with that forecast

for 3 days, 5 days, and the 7-day forecast were also calculated.

In Deng et al [12], an RNN-based LSTM deep learning model was combined with the SIRJD compartmental model was used. The main agenda of the work is to predict the transmission rate of the COVID pandemic in the US, and using the predicted transmission rate, the trajectory of the disease was predicted for the next 35 and 42 days. In Bousquet et al. [13], a neural network based on LSTM was implemented on the SIRD model of the coronavirus, the transmission and death rate was predicted along with that the 10-week trajectory for all the compartments. This analysis was done for France, the United Kingdom, Germany, and South Korea. In Deng et al. [14], DNN (deep neural network) and RNN with LSTM have been considered, and they were applied to the SIRD model of the omicron virus to predict the transmission parameters. and based on those parameters, the next 28-day trajectory was predicted, and this analysis was carried out in various cities in China, such as Shanghai, Taiwan, and Hong Kong.

In Hu et al. [15], a modified version of PINN was used to predict various transmission parameters for the SICRD model of COVID-19 and, using the predicted parameters, the next 90-day trajectory for the C and D compartments were predicted, where before the prediction, the data was pre-processed using the wavelet transform. Along with that transmission parameters were predicted with data of 90 days of various cities in the US. It was also shown that the proposed PINN model described in the work is better than the conventional PINN.

In Bhujju et al. [16] the temperature dependence of the transmission rate has been studied using the SEIR model for humans and the LSEI model for mosquitoes. Various mathematical analyses, such as the stability of disease-free equilibrium, and the existence of endemic equilibrium have been done. Numerical results have been carried out using various temperatures and it was observed that temperature plays a huge role in the transmission rate. In Keno et al . [17] the temperature dependency of the transmission, parameter is studied using the SIR model for humans and the SI model for mosquitoes various mathematical analyses such as the local stability of the equilibrium points and global stability of the equilibrium points were performed and it was also proved that if the basic reproduction number is less than one, then the DFE is locally and globally asymptotically stable. Finally, the influence of the temperature on the transmission was studied and it was concluded that temperature plays a significant role in the transmission of the disease.

In Proctor et al. [18] DMD (dynamic model decomposition) was used to incorporate the effect of control to extract low-order models from high-dimensional, complex systems. In Alla and Kutz. [19] DMD is implemented to reduce the order of a nonlinear dynamical system. In Andreuzzi et al. [20] an extension of DMD is used for forecasting the future states of parametric dynamical systems. In Watson et al. [21], the Bayesian time series model has been implemented along with random forest to predict the number of cases and deaths using the SIRD compartmental model. Along with that, the 21-day forecast has been done on three different cities namely New York, Colorado, and West Virginia. More works on the malaria mathematical model can be found in [22–29].

Most of the works that have been carried out till now related to understanding the dynamics of malaria transmission consist of purely mathematical modeling. But this work makes use of the methods of deep learning in analyzing the dynamics of malaria transmission. One of the reasons why the deep learning method is used instead of other methods is because deep learning models are built to resemble the human brain, enabling them to capture complex patterns in data, This unique property makes them more suitable for modeling malaria dynamics.

In this work, a simple ANN is used to predict the trajectory of all five compartments of the model. To predict the parameters associated with malaria transmission ANN, CNN, and RNN are used. The main reason why RNN was used is because RNN forecasts the future value of a quantity by storing large

amounts of past data. Finally, using DMD, the risk of the disease was calculated and the main reason why DMD is used is because DMD can draw insights from raw data, unlike other deep learning methods. The main entity that controls the transmission of a disease is the transmission rate and thus in this work, the transmission rate of disease is analyzed considering the temperature and height simultaneously.

This work is divided in the following manner. In section 2 the model related to disease transmission has been formulated. In section 3 the problem statement, the methodology, and the results are discussed. Section 4 is devoted to concluding remarks and future directions.

2 Model formulation

In this section, we formulate our model. Both human and mosquito populations are considered in the model since malaria involves two different species mosquitoes and humans. This methodology analyzes the population of humans and mosquitoes using compartment models. The human compartment is divided into three compartments susceptible, infected, and recovered (S, I, R) and the mosquito compartment is divided into two compartments which are susceptible and infected (S, I). This is a two-species system thus the population of one of the species is affected by the other. More precisely when infected mosquitoes come in contact with susceptible humans it leads to an increase in the population of infected humans, in the same way when infected humans come in contact with susceptible mosquitoes it leads to an increase in the population of infected mosquitoes. Figure 2 explains the interaction between the human and mosquito population.

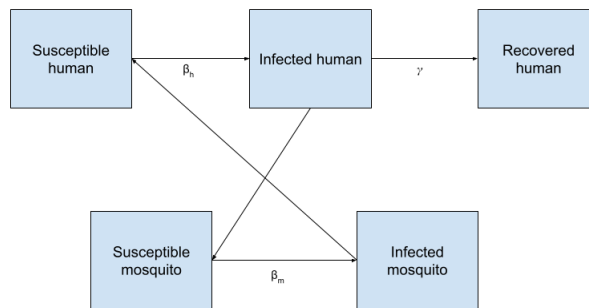


Figure 2: Schematic diagram of SIR-SI system

For the human population, we consider the standard SIR model, and for the mosquito population, we consider the SI model, the following is the system of differential equations.

$$\begin{aligned}
\frac{dS_h}{dt} &= \Gamma_h N_h - \frac{\beta_h S_h I_m}{N_h} - \mu_h S_h \\
\frac{dI_h}{dt} &= \frac{\beta_h S_h I_m}{N_h} - (\gamma_h + \mu_h) I_h \\
\frac{dR_h}{dt} &= \gamma_h I_h - \mu_h R_h \\
\frac{dS_m}{dt} &= \Gamma_m N_m - \frac{\beta_m S_m I_h}{N_m} - \mu_m S_m \\
\frac{dI_m}{dt} &= \frac{\beta_m S_m I_h}{N_m} - \mu_m I_m.
\end{aligned} \tag{2.1}$$

The model used in this work is the SIR-SI model. The SIR model is used for the human population and the SI model is used for the mosquito population. Table 1 and 2 explain the compartments and the parameters used.

Compartment Symbol	Explanation
S_h	It represents the section of the human population who are susceptible to malaria
I_h	It represents the section of humans who are infected with malaria
R_h	It represents the section of humans who have recovered from malaria
S_m	It represents the section of mosquitoes that are susceptible to the malaria-causing parasite
I_m	It represents the section of mosquitoes that are infected with the malaria-causing parasite

Table 1: Interpretation of compartments

Compartment Symbol	Explanation
Γ_h	Birth rate of the humans
N_h	Total human population
β_h	Transmission of malaria in humans
μ_h	mortality rate of humans due to malaria
γ_h	recovery rate of humans
Γ_m	Birth rate of mosquitoes
β_m	transmission of malaria in mosquitoes
μ_m	mortality rate of mosquitoes
N_m	Total population of mosquitoes

Table 2: Parameters description

2.1 Disease-free steady state analysis

In this section, we perform the steady state analysis. Steady-state solutions play an important role when analytical solution is not known and we want to study the qualitative properties of solutions.

We define the basic reproduction number for the model (3.1) as

$$R_0 = \frac{\beta_h \beta_m \Gamma_h \Gamma_m}{\mu_h \mu_m^2 (\mu_h + \gamma_h)}.$$

Observe that the basic reproduction number depends on recruitment rates, infection rates, recovery rates, and mortality rates.

Theorem 2.1. *If $R_0 < 1$, then the disease-free steady state is locally stable*

Proof. For the analysis of the disease-free steady state, we need to equate the infected and recovered population of both species to zero and thus we get $S_h = \frac{\Gamma_h}{\mu_h}$, $I_h = 0$, $R_h = 0$, $S_m = \frac{\Gamma_m}{\mu_m}$, $I_m = 0$.

Dividing the first three equations N_h and the last two equations with N_m in (3.1), we get

$$\begin{aligned} \frac{dS_h}{dt} &= \Gamma_h - m\beta_h S_h I_m - \mu_h S_h \\ \frac{dI_h}{dt} &= m\beta_h S_h I_m - (\gamma_h - \mu_h) I_h \\ \frac{dR_h}{dt} &= \gamma_h I_h - \mu_h R_h \\ \frac{dS_m}{dt} &= \Gamma_m - \frac{\beta_m S_m I_h}{m} - \mu_m S_m \\ \frac{dI_m}{dt} &= \frac{\beta_m S_m I_h}{m} - \mu_m I_m. \end{aligned} \tag{2.2}$$

Now our task is to linearise the system (2.2) around the disease-free steady state. After linearization, we obtain the following system

$$\begin{aligned} \frac{dS_h}{dt} &= \Gamma_h - m\beta_h \frac{\Gamma_h}{\mu_h} I_m - \mu_h S_h \\ \frac{dI_h}{dt} &= m\beta_h \frac{\Gamma_h}{\mu_h} I_m - (\gamma_h + \mu_h) I_h \\ \frac{dR_h}{dt} &= \gamma_h I_h - \mu_h R_h \\ \frac{dS_m}{dt} &= \Gamma_m - \beta_m \frac{\Gamma_m}{m\mu_m} I_h - \mu_m S_m \\ \frac{dI_m}{dt} &= \frac{\Gamma_m \beta_m I_h}{m\mu_m} - \mu_m I_m. \end{aligned}$$

Constructing the Jacobian matrix, we get

$$J = \begin{bmatrix} -\mu_h & 0 & 0 & 0 & -\frac{m\beta_h\Gamma_h}{\mu_h} \\ 0 & -(\gamma_h + \mu_h) & 0 & 0 & \frac{m\beta_h\Gamma_h}{\mu_h} \\ 0 & \gamma_h & -\mu_h & 0 & 0 \\ 0 & \frac{-\beta_m\Gamma_m}{m\mu_m} & 0 & -\mu_m & 0 \\ 0 & \frac{\beta_m\Gamma_m}{m\mu_m} & 0 & 0 & -\mu_m \end{bmatrix}.$$

The characteristic polynomial of the above matrix is

$$f(\lambda) = -(\lambda + \mu_h)(\lambda + \mu_h)(\lambda + \mu_m)\left[(\lambda + \mu_m)(\lambda + \mu_h + \gamma_h) - \frac{\beta_h\beta_m\Gamma_h\Gamma_m}{\mu_h\mu_m}\right].$$

For the system to be stable, all the eigenvalues must be negative real parts. It is clear that three of the eigenvalues are negative; we need to check the roots of the quadratic polynomial for the remaining two eigenvalues.

Now by solving the quadratic equation, we get the roots as

$$\frac{-(\gamma + \mu_h + \mu_m) + \sqrt{(\mu_m + \mu_h + \gamma_h)^2 - 4(\mu_m(\mu_h + \gamma_h) - \frac{\beta_h\beta_m\Gamma_h\Gamma_m}{\mu_h\mu_m})}}{2}$$

$$\frac{-(\gamma + \mu_h + \mu_m) - \sqrt{(\mu_m + \mu_h + \gamma_h)^2 - 4(\mu_m(\mu_h + \gamma_h) - \frac{\beta_h\beta_m\Gamma_h\Gamma_m}{\mu_h\mu_m})}}{2}.$$

If we observe, the second root is again always negative, and thus we need to find out the condition for which the first root is negative and that is

$$\mu_m(\mu_h + \gamma_h) - \frac{\beta_m\beta_h\Gamma_m\Gamma_h}{\mu_h\mu_m} > 0.$$

Rearranging the above inequality, we get the expression

$$\frac{\beta_h\beta_m\Gamma_h\Gamma_m}{\mu_h\mu_m^2(\mu_h + \gamma_h)} < 1.$$

So, if $R_0 < 1$, it will ensure us that the disease-free steady state is stable. \square

2.2 Endemic steady state analysis

In this subsection, we aim to study the stability of the endemic steady-state. Given system of equations is

$$\begin{aligned}\frac{dS_h}{dt} &= \Gamma_h - m\beta_h \frac{\Gamma_h}{\mu_h} I_m - \mu_h S_h \\ \frac{dI_h}{dt} &= m\beta_h \frac{\Gamma_h}{\mu_h} I_m - (\gamma_h + \mu_h) I_h \\ \frac{dR_h}{dt} &= \gamma_h I_h - \mu_h R_h \\ \frac{dS_m}{dt} &= \Gamma_m - \beta_m \frac{\Gamma_m}{m\mu_m} I_h - \mu_m S_m \\ \frac{dI_m}{dt} &= \frac{\Gamma_m \beta_m I_h}{m\mu_m} - \mu_m I_m.\end{aligned}$$

Before proceeding with the next theorem it is essential to define the following quantities

$$\begin{aligned}b &= \mu_h + \frac{\beta_h I_m^*}{N_h} + \mu_h + \gamma + \frac{\beta_h I_h^*}{N_m} + \mu_m \\ c &= (\mu_h + \frac{\beta_h I_m^*}{N_h})(\mu_h + \gamma) + (\mu_h + \gamma)(\frac{\beta_h I_h^*}{N_m} + \mu_m) + (\frac{\beta_h I_h^*}{N_m} + \mu_m)(\mu_h + \frac{\beta_h I_m^*}{N_h}) - \frac{\beta_m \beta_h S_m^* S_h^*}{N_m N_h} \\ d &= \left(\mu_h + \frac{\beta_h I_m^*}{N_h}\right) \left[(\mu_h + \gamma)(\frac{\beta_h I_h^*}{N_m} + \mu_m) - \frac{\beta_m \beta_h S_m^* S_h^*}{N_m N_h} + \frac{\beta_m \beta_h^2 S_m^* S_h^* I_m^*}{N_m N_h^*} \right],\end{aligned}$$

where $S_m^*, S_h^*, I_m^*, I_h^*$ are the non trivial equilibrium solutions.

Theorem 2.2. *If $R_0 > 1$ and if $b, c, d, bc - d > 0$ then the endemic steady state is locally stable.*

Proof. The equilibrium points will be obtained by equating all of the above time derivatives to zero and by solving them for non-trivial solutions, we obtain the solutions as

$$\begin{aligned}S_h^* &= \frac{N_h(\gamma + \mu_h)(\mu_m N_m + \frac{\Gamma_h N_h \beta_m}{\gamma + \mu_h})}{\beta_m(\mu_h N_h + \frac{\Gamma_m N_m \beta_h}{\mu_m})} \\ I_h^* &= \frac{N_h N_m \mu_m \mu_h (R_0 - 1)}{\beta_m(\mu_h N_h + \frac{\Gamma_m N_m \beta_h}{\mu_m})} \\ R_h^* &= \frac{N_h N_m \mu_m \gamma_h (R_0 - 1)}{\beta_m(\mu_h N_h + \frac{\Gamma_m N_m \beta_h}{\mu_m})} \\ S_m^* &= \frac{N_m \mu_m (\mu_h N_h + \frac{\Gamma_m N_m \beta_h}{\mu_m})}{\beta_h(\mu_m N_m + \frac{\Gamma_h N_h \beta_m}{\gamma + \mu_h})} \\ I_m^* &= \frac{N_h N_m \mu_m \mu_h (R_0 - 1)}{\beta_h(\mu_m N_m + \frac{\Gamma_h N_h \beta_m}{\gamma + \mu_h})}.\end{aligned}$$

Linearizing the model (2.2) around the endemic equilibrium point, we get the following system

$$\begin{aligned}
\frac{dS_h}{dt} &= \Gamma_h N_h - \frac{\beta_h}{N_h} (S_h^* I_m + I_m^* S_h - S_h^* I_m^*) - \mu_h S_h \\
\frac{dI_h}{dt} &= \frac{\beta_h}{N_h} (S_h^* I_m + I_m^* S_h - S_h^* I_m^*) - \gamma I_h - \mu_h I_h \\
\frac{dR_h}{dt} &= \gamma I_h - \mu_h R_h \\
\frac{dS_m}{dt} &= \gamma_m N_m - \frac{\beta_m}{N_m} (S_m^* I_h + S_m I_h^*) - \mu_m S_m \\
\frac{dI_m}{dt} &= \frac{\beta_m}{N_m} (S_m^* I_h + S_m I_h^*) - \mu_m I_m.
\end{aligned}$$

Writing the Jacobian matrix, we get

$$J = \begin{bmatrix}
-\frac{\beta_h I_m^*}{N_h} - \mu_h & 0 & 0 & 0 & -\frac{\beta_h S_h^*}{N_h} \\
\frac{\beta_h I_m^*}{N_h} & -(\gamma_h + \mu_h) & 0 & 0 & \frac{\beta_h S_h^*}{N_h} \\
0 & \gamma_h & -\mu_h & 0 & 0 \\
0 & -\frac{\beta_h S_m^*}{N_m} & 0 & -\frac{\beta_h S_m^*}{N_m} - \mu_m & 0 \\
0 & \frac{\beta_h S_m^*}{N_m} & 0 & \frac{\beta_h S_m^*}{N_m} & -\mu_m
\end{bmatrix}$$

The characteristic polynomial of the above matrix is

$$f(\lambda) = -(\lambda + \mu_h)(\lambda + \mu_m) \left(\left[\lambda + \mu_h + \frac{\beta_h I_m^*}{N_h} \right] \left[(\lambda + \mu_h + \gamma) \left(\lambda + \frac{\beta_m I_h^*}{N_m} + \mu_m \right) - \frac{\beta_m \beta_h S_m^* S_h^*}{N_h N_m} \right] + \frac{\beta_h^2 \beta_m S_h^* I_m^* S_m^*}{N_h^2 N_m} \right).$$

From the above equation, we can see that we have two linear factors and a cubic factor.

The cubic factor could be analyzed using the following theorem:

Lemma 2.3. *Let $f(x) = ax^3 + bx^2 + cx + d$ be a cubic polynomial. For $f(x)$ to have all negative roots or complex roots with negative real parts, the following conditions are necessary:*

$$a > 0, b > 0, c > 0, d > 0, bc - ad > 0.$$

Now by using the above-stated lemma, we can arrive at our required result □

2.3 Temperature and altitude dependence of the transmission rate

The transmission rate of the disease is heavily dependent on the altitude of the place as well as the temperature of the place and thus to consider both of the factors we write.

$$\beta(T, h) = \beta_0 e^{-\frac{(T-25)^2}{\eta^2}} e^{-\frac{h^2}{\xi^2}} (1 - e^{-\frac{h^2}{\xi^2}}), \tag{2.3}$$

where β_0 is the transmission constant of the region, T is the temperature of the place, h is the height of the place, η and ξ are the constants associated with the region's temperature and height respectively.

Here $e^{-\frac{(T-25)^2}{\eta^2}}$ is used to model the temperature and $e^{-\frac{h^2}{\xi^2}}(1 - e^{-\frac{h^2}{\xi^2}})$ is used to model the height. The main reason for considering the above two functions is the following

Temperature:

Malaria transmission will be very minimal when the temperature is either extremely high or it is extremely low and thus to model this variation the Gaussian function is used and the reason for shifting it by 25 is because the optimum temperature for mosquito's existence and malaria transmission is 25 °C.

Altitude:

Malaria transmission is completely zero when the altitude is zero since there won't be any mosquitoes in the sea and in the same way when the altitude is extremely high again the transmission is completely zero since there are no mosquitoes in the space and thus to model both of these conditions the negative exponential function is used in this manner.

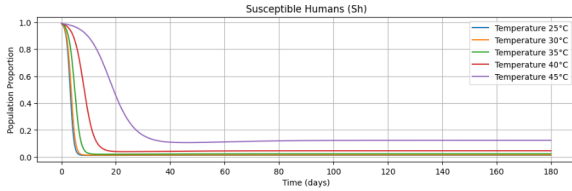
Assuming the temperature is from T_1 to T_2 and the height is from h_1 to h_2 , we can write

$$\beta_{avg} = \int_{T_1}^{T_2} \int_{h_1}^{h_2} e^{-\frac{(T-25)^2}{\eta^2}} e^{-\frac{h^2}{\xi^2}} (1 - e^{-\frac{h^2}{\xi^2}}) dh dT. \tag{2.4}$$

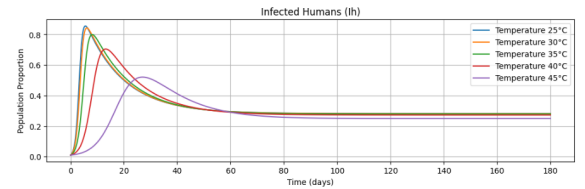
Here the effect of transmission rate is studied by changing the temperature values for a fixed height. The parameters considered are the following:

$\beta_0 = 10$, and for human we have taken $\eta = 200, \xi = 20000$ and for mosquitoes, $\eta = 400, \xi = 40000$. The different temperatures which are used are 25°, 30°, 35°, 40°, 45°.

The effect of temperature on the transmission rate while maintaining a height of 75 m can be observed in Figures 3 and 4, while the effect at a height of 100 m is shown in Figures 5 and 6, and at a height of 125 m in Figures 7 and 8.

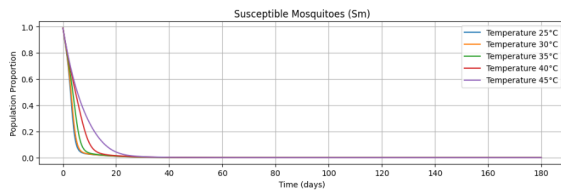


(a) Susceptible human

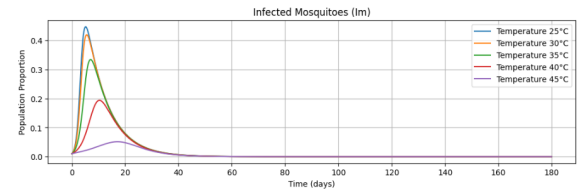


(b) Infected human

Figure 3: Effect on human population when height is 75 m

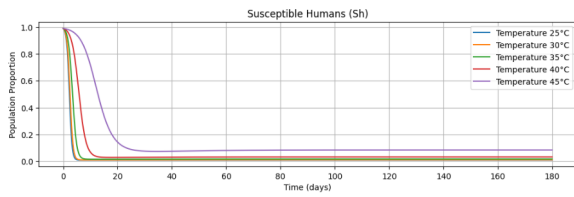


(a) Susceptible mosquito

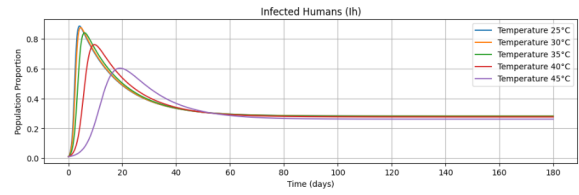


(b) Infected mosquito

Figure 4: Effect on mosquitoes population when height is 75 m

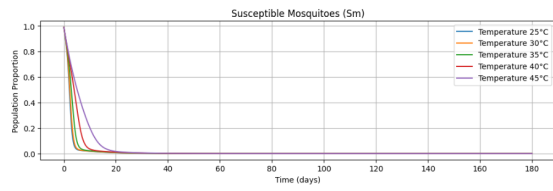


(a) Susceptible human

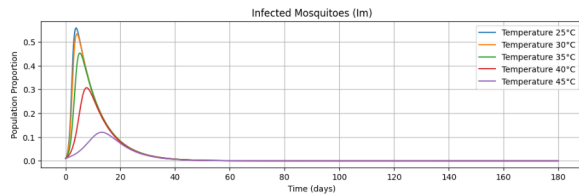


(b) Infected human

Figure 5: Effect on human population when height is 100 m

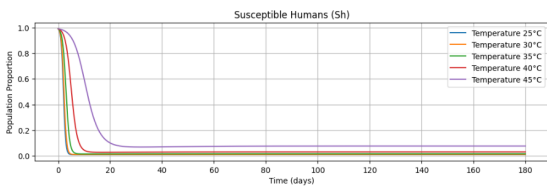


(a) Susceptible mosquito

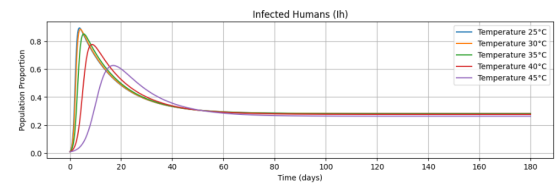


(b) Infected mosquito

Figure 6: Effect on mosquitoes population when height is 100 m

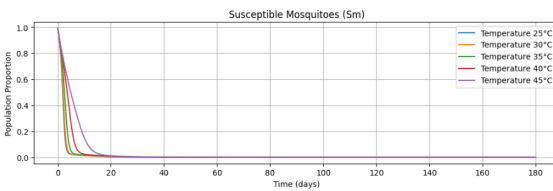


(a) Susceptible human

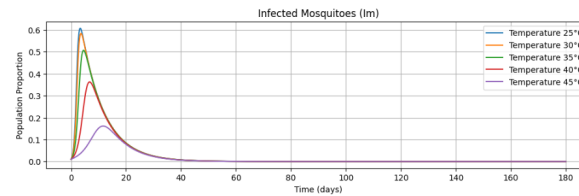


(b) Infected human

Figure 7: Effect on human population when height is 125 m



(a) Susceptible mosquito



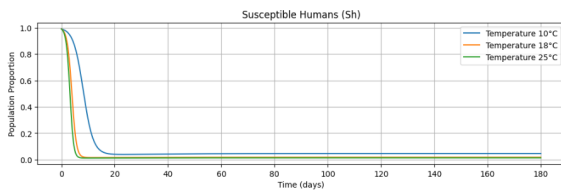
(b) Infected mosquito

Figure 8: Effect on mosquito population when height is 125 m

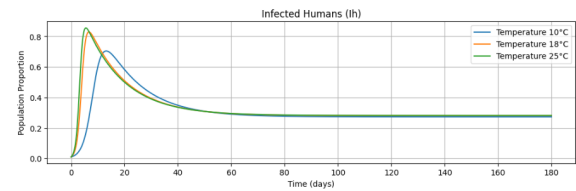
Thus in this graph, we have plotted the graphs for various temperatures and we can observe that the transmission rate is the maximum for 25° which is the least of all the temperatures.

We verify if 25° is the optimal temperature. We consider the following values for temperature $10^\circ, 18^\circ, 25^\circ$.

The effect of temperature on the transmission rate while maintaining a height of 75 m can be observed in Figures 9 and 10, while at a height of 100 m, it can be observed in Figures 11 and 12, and at a height of 125 m in Figures 13 and 14.

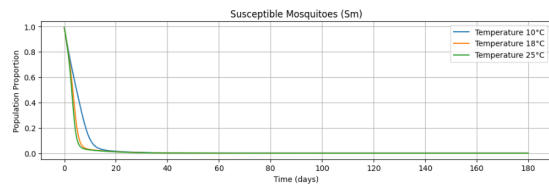


(a) Susceptible human

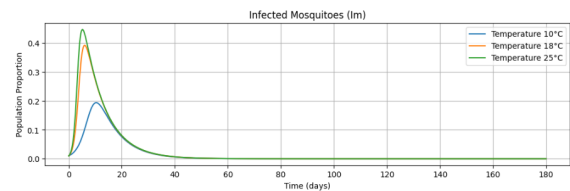


(b) Infected human

Figure 9: Effect on human population when height is 75 m

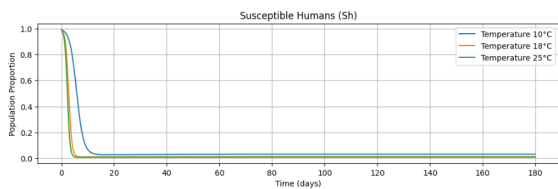


(a) Susceptible mosquito

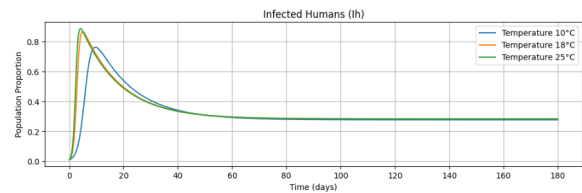


(b) Infected mosquito

Figure 10: Effect on mosquito population when height is 75 m

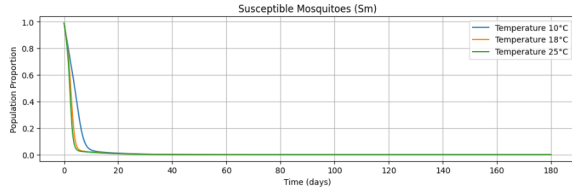


(a) Susceptible human

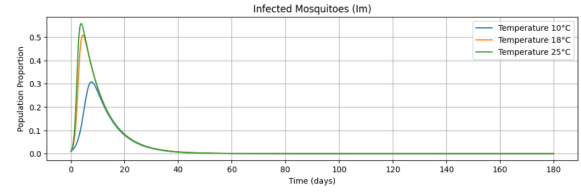


(b) Infected human

Figure 11: Effect on human population when height is 100 m

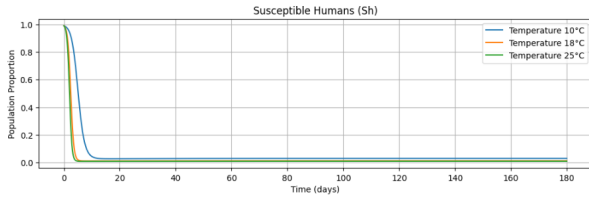


(a) Susceptible mosquito

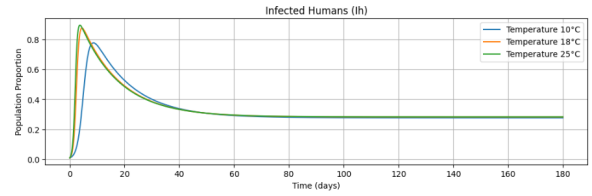


(b) Infected mosquito

Figure 12: Effect on mosquito population when height is 100 m

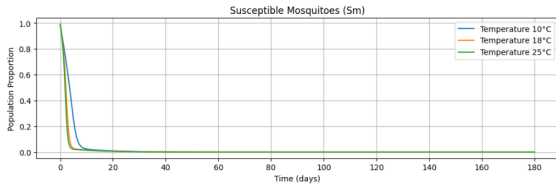


(a) Susceptible human

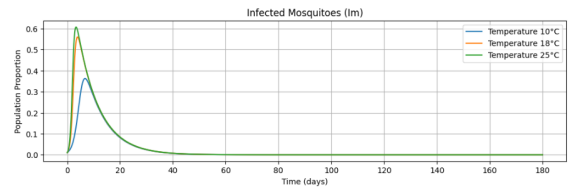


(b) Infected human

Figure 13: Effect on human population when height is 125 m



(a) Susceptible mosquito



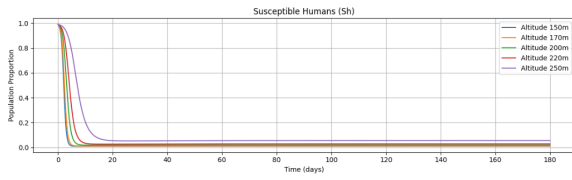
(b) Infected mosquito

Figure 14: Effect on mosquito population when height is 125 m

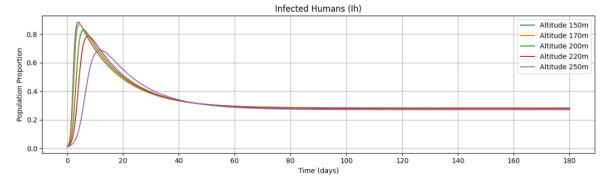
Again, we can observe that the transmission is the highest when the temperature is 25° which is the highest of all temperatures. Thus the threshold value of the temperature is 25° and the transmission rate is the highest only when the temperature is 25° . The main reason why this happens is that the temperature component is $e^{-\frac{(T-25)^2}{\eta^2}}$, and this component achieves the maximum value when $T = 25^\circ$.

Here transmission is analyzed by keeping the temperature constant and varying the height. Values of altitude used are 150, 170, 200, 220, and 250 m.

The effect of height on the transmission rate can be observed under different temperatures: at 28° in Figures 15 and 16, at 35° in Figures 17 and 18, and at 42° in Figures 19 and 20.

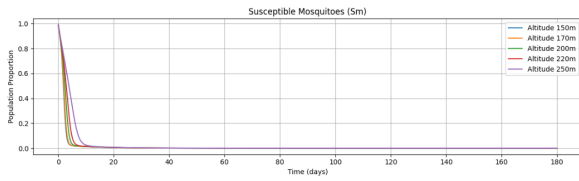


(a) Susceptible humans

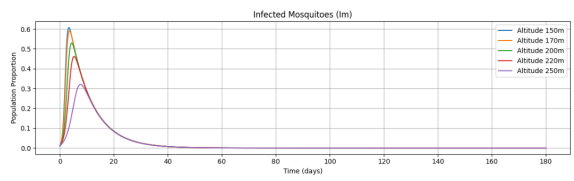


(b) Infected human

Figure 15: Dynamics of human population when temperature is 28 degrees Celsius

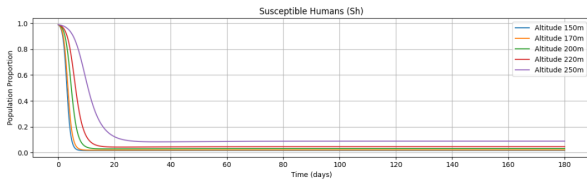


(a) Susceptible mosquito

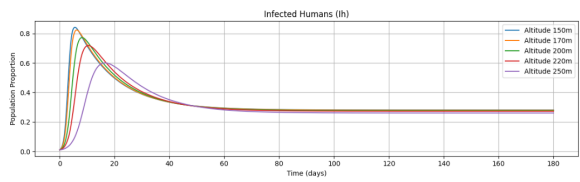


(b) Infected mosquito

Figure 16: Dynamics of mosquito population when temperature is 28 degrees Celsius

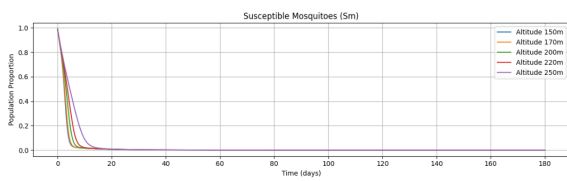


(a) Susceptible human

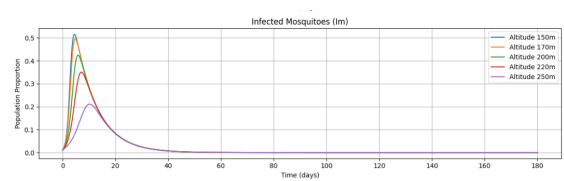


(b) Infected human

Figure 17: Dynamics of human population when temperature is 35 degrees Celsius

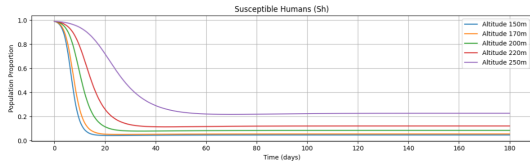


(a) Susceptible mosquito

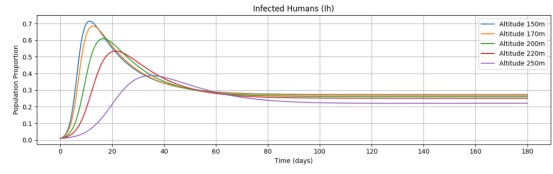


(b) Infected mosquito

Figure 18: Dynamics of mosquito population when temperature is 35 degrees Celsius

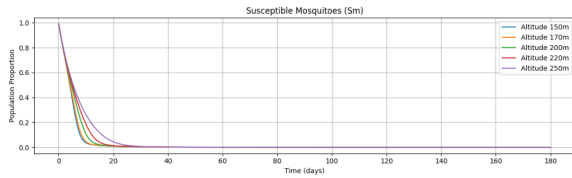


(a) Susceptible human

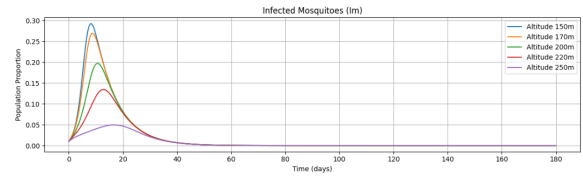


(b) Infected human

Figure 19: Dynamics of human population when temperature is 42 degrees Celsius



(a) Susceptible mosquito



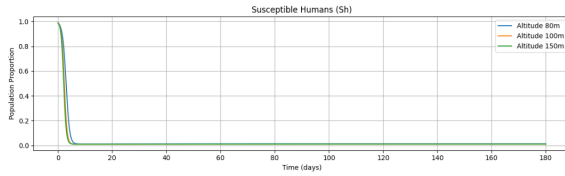
(b) Infected mosquito

Figure 20: Dynamics of mosquito population when temperature is 42 degrees Celsius

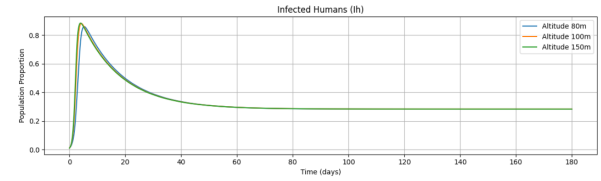
Here we observe that the transmission achieves its highest value when the height is 150m, which is the least value among the chosen values.

To make sure 150 m is the threshold value for the altitude. Here values of altitude considered are 80 m and 100 m.

The effect of height on the transmission rate while maintaining a constant temperature of 28° can be observed in Figures 21 and 22, while at 35° it can be seen in Figures 23 and 24, and at 42° in Figures 25 and 26

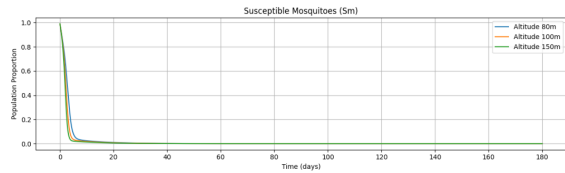


(a) Susceptible humans

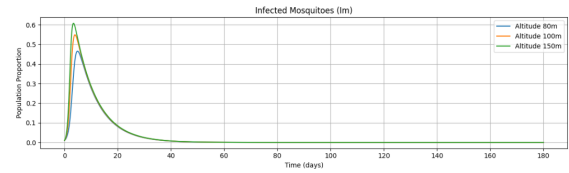


(b) Infected human

Figure 21: Dynamics of human population when temperature is 28 degrees Celsius

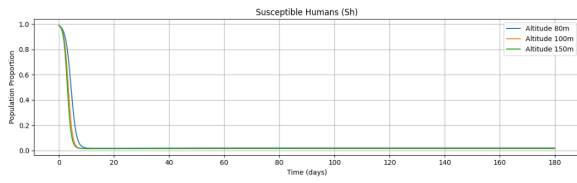


(a) Susceptible mosquito

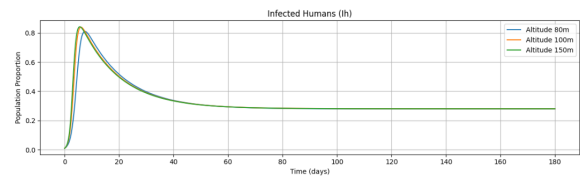


(b) Infected mosquito

Figure 22: Dynamics of mosquito population when temperature is 28 degrees Celsius

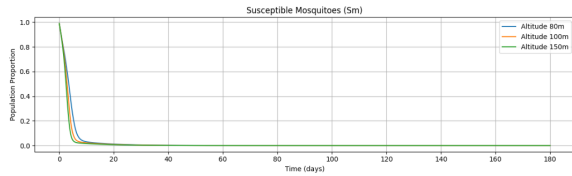


(a) Susceptible human

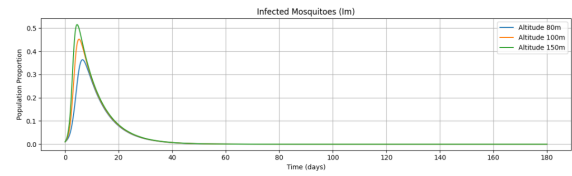


(b) Infected human

Figure 23: Dynamics of human population when temperature is 35 degrees Celsius

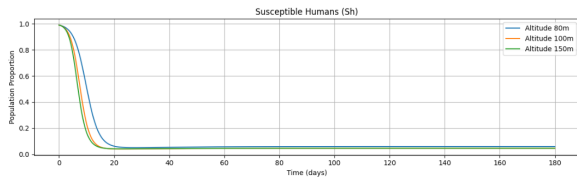


(a) Susceptible mosquito

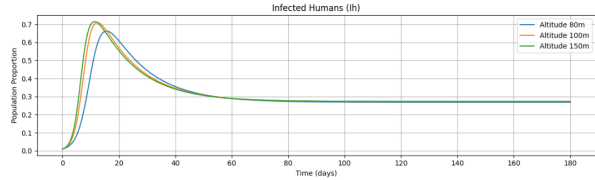


(b) Infected mosquito

Figure 24: Dynamics of mosquito population when temperature is 35 degrees Celsius

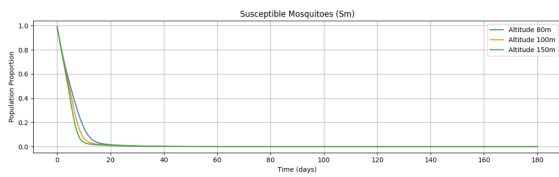


(a) Susceptible human

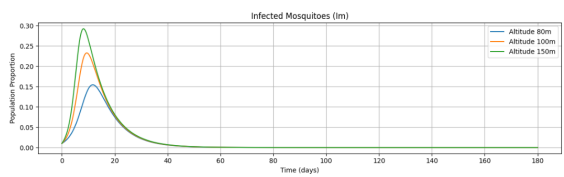


(b) Infected human

Figure 25: Dynamics of human population when temperature is 42 degrees Celsius



(a) Susceptible mosquito



(b) Infected mosquito

Figure 26: Dynamics of mosquito population when temperature is 42 degrees Celsius

Thus we observe that the transmission rate is the highest when the height is 150 and in this case, it is the highest value among the chosen values thus from this we can conclude that $h = 150$ is the threshold value for the altitude. The function $f(h) = e^{-\frac{h^2}{\xi^2}} (1 - e^{-\frac{h^2}{\xi^2}})$ achieves its highest value when $h = \xi \sqrt{\ln(2)}$ and thus the transmission rate increases as the value of height approaches $h = \xi \sqrt{\ln(2)}$.

By substituting both the values of ξ and taking the average we get approximately 142.1 thus the optimal value for altitude can be concluded to be in the range 140 – 150 and since it can be observed that the

trajectory for all of these values is nearly the same.

3 Numerical Simulation and Deep Learning

Whenever there is a disease transmission in a particular country or state, there is a significant number of deaths and sufferings that the people of the place have to undergo. One of the main reasons why this happens is when the spread of the disease goes uncontrollably. In this work, the following problem statements are addressed to understand the transmission of disease.

3.1 Predicting the trajectory of the compartments

Whenever there is a disease transmission in a country/state the medical professionals and the government professionals should be prepared to handle the situation and to provide different levels of support such as vaccination, hospital facilities, implementing curfews, etc. Knowing the trajectory will enable the government to make more precise decisions. The overall methodology for this problem statement can be found in Figure 27.

Here the neural network is used to make a recursive relation between the trajectory at $t = n$ and trajectory $t = n + 1$. The main reason why neural network is used is because it has a unique ability to identify nonlinear relations in the data.

Following are the parameters that are used for predicting the trajectory:

β_h	β_m	γ	μ_h	Γ_h	μ_m	Γ_m
0.9	0.8	0.05	0.02	0.02	0.2	0.08

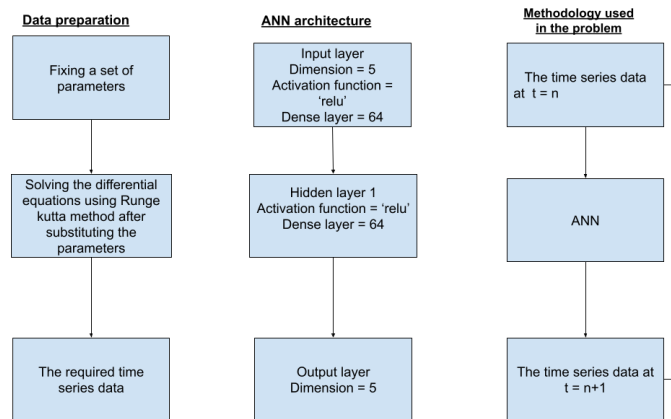


Figure 27: Neural network architecture and methodology

Here the neural network is used to make a recursive relation between the trajectory at $t = n$ and trajectory $t = n + 1$. Neural network is mainly used because of its unique ability to identify nonlinear relations in the data. The predicted and the actual trajectories are shown in Figure 28 - Figure 29.

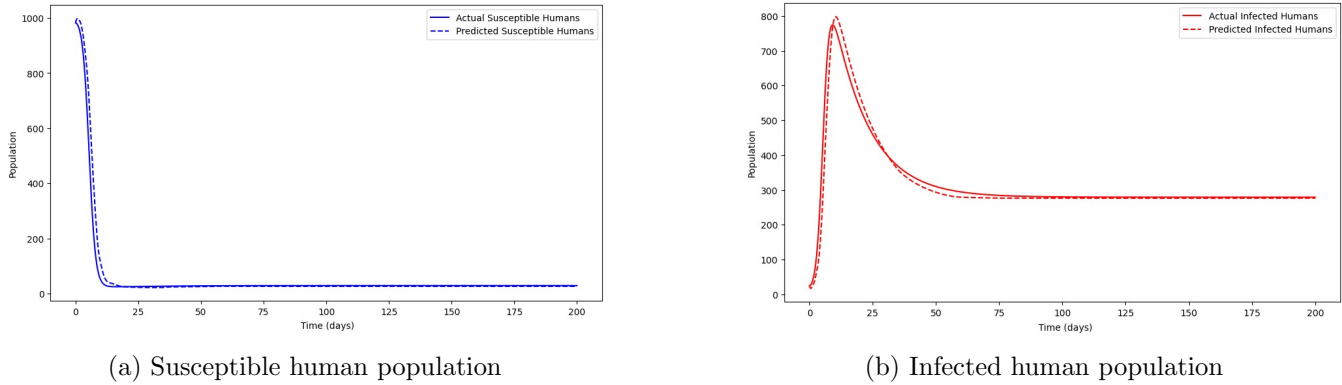


Figure 28: Comparison of predicted and actual trajectories for susceptible and infected human population.

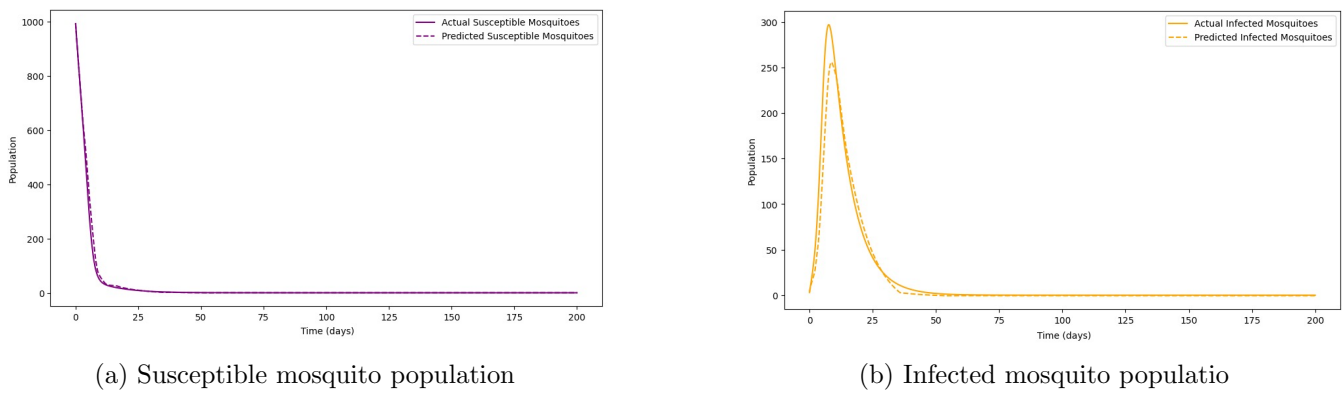


Figure 29: Comparison of predicted and actual trajectories for susceptible and infected mosquito population.

Now every compartment has two factors one is called the incoming factor which means the factors that lead to an increase in the compartment's population. The other one is the outgoing factor which leads to a decrease in the compartment's population.

In the susceptible compartment, there is only one incoming factor which is the birth rate, and where there are two outgoing factors namely the death rate and the interaction with the infected population this can be easily observed from . Since the number of outgoing factors is more than the number of incoming factors the susceptible population decreases with time.

Similar to the susceptible compartment the infected compartment also has only one incoming factor which is the interaction between the susceptible population and two outgoing factors which are the death rate and the recovery rate. Thus when an infection spreads in a place the number of infected people increases but as time passes the people develop immunity to the disease and thus the infected population

decreases after reaching a threshold value.

From the flow chart of the compartment model, we can observe that the transfer of people is from susceptible to infected. Thus we can observe a sudden drop in the susceptible people and a huge rise in the infected compartment at the same time.

3.2 PREDICTING THE TRANSMISSION RATE OF THE DISEASE

The main factors that control the dynamics of a disease system are the parameters associated with it. Thus knowing the parameters of disease will enable the medical professionals to know the movement of people from one compartment to the other and it will provide them with a good clarity of what measures must be taken. To address this problem statement three different architectures of neural networks are used in this work they are ANN, CNN, and RNN. The complete overview of the problem can be seen in Figure 30

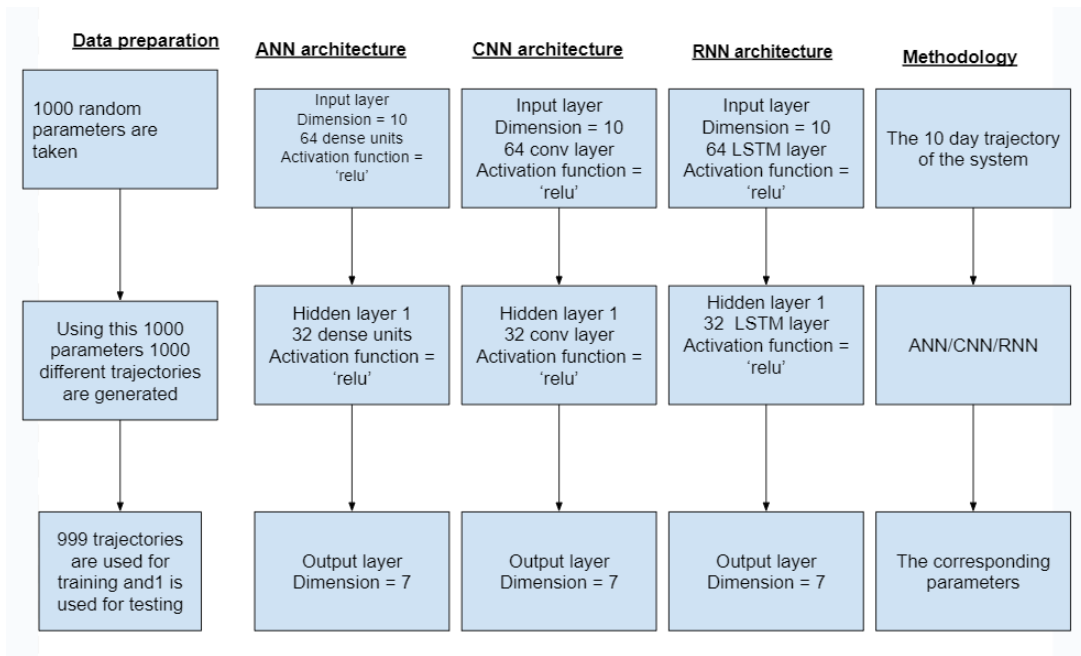


Figure 30: Details of neural network architecture and methodology

The number of layers for each model is kept the same for a novel comparison. Here the main reason why one trajectory is used for testing is because every disease transmission is always associated with one trajectory and one set of parameters. The results from each of the neural networks can be found in 3, 4, 5 .

Parameters	Predicted value	Actual value	Error
Birth rate of humans	0.056	0.044	28.6 %
Transmission rate of humans	0.227	0.264	14.07 %
Death rate of human	0.442	0.451	1.86 %
Recovery rate of humans	0.378	0.379	0.32 %
Birth rate of mosquitoes	0.450	0.444	1.37 %
Transmission rate in mosquitoes	0.242	0.241	0.40 %
Death rate of mosquitoes	0.3806	0.3807	0.04 %

Table 3: Parameter prediction using ANN

Parameters	Predicted value	Actual value	Error
Birth rate of humans	0.1904	0.1784	6.69 %
Transmission rate of humans	0.264	0.297	11.11 %
Death rate of human	0.428	0.433	1.02 %
Recovery rate of humans	0.1605	0.1602	0.17 %
Birth rate of mosquitoes	0.223	0.217	2.96 %
Transmission rate of mosquitoes	0.284	0.274	3.54 %
Death rate of mosquitoes	0.479	0.481	0.24 %

Table 4: Parameter prediction using CNN

Parameters	Predicted value	Actual value	Error
Birth rate of humans	0.172	0.169	1.44 %
Transmission rate of humans	0.111	0.103	8.21 %
Death rate of human	0.0854	0.0841	1.58 %
Recovery rate of humans	0.492	0.495	0.17 %
Birth rate of mosquitoes	0.445	0.457	2.47 %
Transmission rate of mosquitoes	0.334	0.338	1.15 %
Death rate of mosquitoes	0.464	0.482	3.38 %

Table 5: Parameter prediction using RNN

For each model, the epoch was set to 10000 to generate the corresponding result and from the comparison, we can conclude that RNN's performance was the best of all the three. The main reason RNN's performance is the best is because RNN can store large amounts of data and make accurate predictions from it compared to the other two neural networks.

3.3 FINDING THE RISK OF A DISEASE

The most important aspect of a disease is the determination of risk. Whenever there is a disease outbreak in a country there are some regions where there is more risk compared to the other regions thus it is essential to calculate this risk of every region. This problem statement is addressed using the method of

DMD (dynamic mode decomposition) and the main reason for using this method is because DMD can make exact predictions from raw data, unlike other deep learning methods. The complete methodology of the problem statement can be seen in Figure 31.

In this work, DMD is used to calculate the disease risk in a particular region. DMD gives the oscillations of the dynamics and thus using the peak values of DMD will give us the overall oscillations of the dynamics which is nothing but the measure of risk. The DMD plot and the eigenvalue spectrum can be found in Figure 32.

From the eigenvalue spectrum, we can observe that all the points are either on or within the unit circle. This shows that the transmission of malaria in Africa is stable. African map with the corresponding color coding based on the risk can be found in Figure 33.

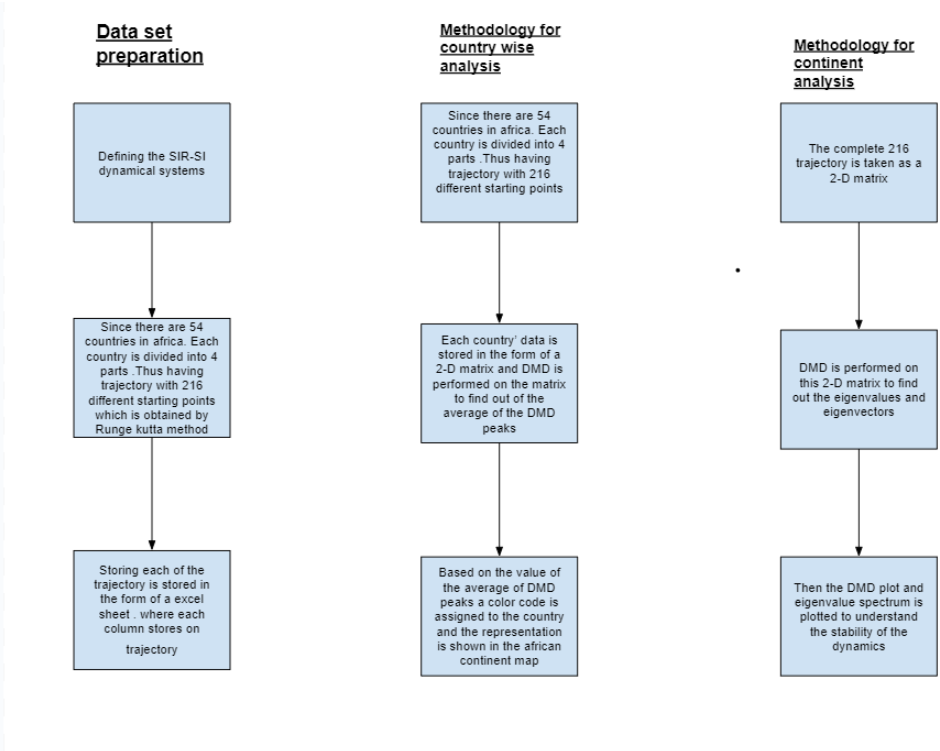
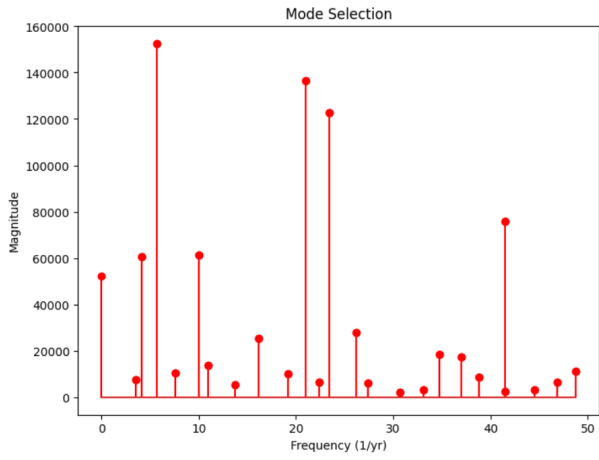
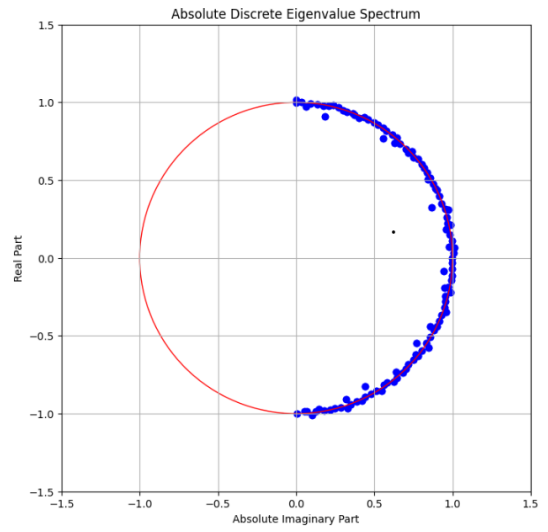


Figure 31: Flow chart of methodology



(a) DMD plot



(b) Infected human

Figure 32: DMD plot and the eigenvalue spectrum

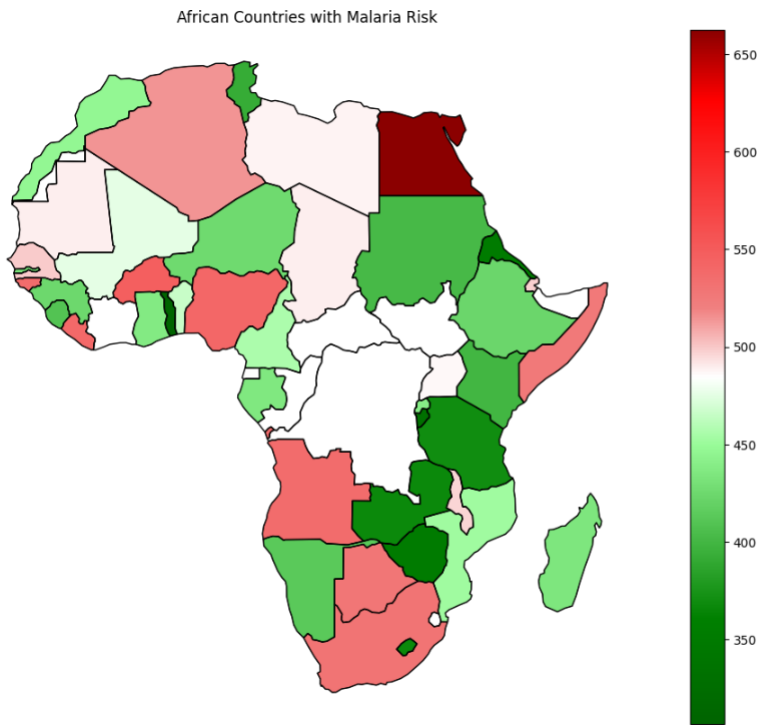


Figure 33: African Map with color coding based on risk

4 Concluding Remarks

In this work, an attempt is made to understand the dynamics of malaria transmission using various mathematical and machine-learning techniques. Using neural networks, the trajectories of all five compartments are predicted, followed by predicting the parameters of disease dynamics using three different architectures of neural networks and finally, this work was concluded by finding the measure of risk using DMD. One thing that could be understood is that disease transmissions are not random processes, but happen under the influence of underlying physical laws.

This work can be deployed by the government of any country to analyze the trajectory of infected people whenever there is a disease outbreak and then predict the future state of the country which will give medical professionals an idea of what kind of measures must be taken to reduce the disease spread

In the future, our idea is to understand the dynamics of malaria using techniques of physics-informed machine learning such as Physics neural networks (PINNs) and Sparse identification of non-linear dynamics (SINDy). We also want to study the stochastic version of this model mainly to study the random fluctuations in the birth and mortality process.

5 Data Availability Statement

This study uses solely synthetic data, which was generated for the purpose of this research. The synthetic data is not based on real-world observations and can be freely accessed. The dataset is available at the link.

References

- [1] Ronald Ross. The prevention of malaria. John Murray, 1911.
- [2] Ronald Ross. Some a priori pathometric equations. *British medical journal*, 1(2830):546, 1915.
- [3] Ronald Ross. An application of the theory of probabilities to the study of a priori pathometry, part i. *Proceedings of the Royal Society of London. Series A, Containing papers of a mathematical and physical character*, 92(638):204–230, 1916.
- [4] Ronald Ross and Hilda P Hudson. An application of the theory of probabilities to the study of a priori pathometry, part iii. *Proceedings of the Royal Society of London. Series A, Containing papers of a mathematical and physical character*, 93(650):225–240, 1917.
- [5] Macdonald G Macdonald. G. The epidemiology and control of malaria. 1957.
- [6] Roy M Anderson and Robert M May. *Infectious diseases of humans: dynamics and control*. Oxford University Press, 1991.
- [7] Sandip Mandal, Ram Rup Sarkar, and Somdatta Sinha. Mathematical models of malaria-a review. *Malaria journal*, 10:1–19, 2011.

- [8] Alonso Ogueda, Erika Martinez, Viswanathan Arunachalam, and Padmanabhan Seshaiyer. Machine learning for predicting the dynamics of infectious diseases during travel through physics-informed neural networks. *Journal of Machine Learning for Modeling and Computing*.
- [9] Enrico Schiassi, Mario De Florio, Andrea D’Ambrosio, Daniele Mortari, and Roberto Furfaro. Physics-informed neural networks and functional interpolation for data-driven parameters discovery of epidemiological compartmental models. *Mathematics*, 9(17):2069, 2021.
- [10] Xiao Ning, Jinxing Guan, Xi-An Li, Yongyue Wei, and Feng Chen. Physics-informed neural networks integrating compartmental model for analyzing covid-19 transmission dynamics. *Viruses*, 15(8):1749, 2023.
- [11] Xiao Ning, Xi-An Li, Yongyue Wei, and Feng Chen. Euler iteration augmented physics-informed neural networks for time-varying parameter estimation of the epidemic compartmental model. *Frontiers in Physics*, 10:1062554, 2022.
- [12] Qi Deng. Dynamics and development of the covid-19 epidemics in the us—a compartmental model with deep learning enhancement. *medRxiv*, pages 2020–05, 2020.
- [13] Arthur Bousquet, William H Conrad, Said Omer Sadat, Nelli Vardanyan, and Youngjoon Hong. Deep learning forecasting using time-varying parameters of the sird model for covid-19. *Scientific Reports*, 12(1):3030, 2022.
- [14] Qi Deng. Modeling the omicron dynamics and development in china: with a deep learning enhanced compartmental model. *medRxiv*, pages 2022–06, 2022.
- [15] Haoran Hu, Connor M Kennedy, Panayotis G Kevrekidis, and Hong-Kun Zhang. A modified pinn approach for identifiable compartmental models in epidemiology with application to covid-19. *Viruses*, 14(11):2464, 2022.
- [16] G Bhujju, GR Phaijoo, and DB Gurung. Mathematical study on impact of temperature in malaria disease transmission dynamics. *Advances in Computer Sciences*, 1(2):1–8, 2018.
- [17] Temesgen Duressa Keno, Oluwole Daniel Makinde, and Legesse Lemecha Obsu. Impact of temperature variability on sirs malaria model. *Journal of Biological Systems*, 29(03):773–798, 2021.
- [18] Joshua L Proctor, Steven L Brunton, and J Nathan Kutz. Dynamic mode decomposition with control. *SIAM Journal on Applied Dynamical Systems*, 15(1):142–161, 2016.
- [19] Alessandro Alla and J Nathan Kutz. Nonlinear model order reduction via dynamic mode decomposition. *SIAM Journal on Scientific Computing*, 39(5):B778–B796, 2017.
- [20] Francesco Andreuzzi, Nicola Demo, and Gianluigi Rozza. A dynamic mode decomposition extension for the forecasting of parametric dynamical systems. *SIAM Journal on Applied Dynamical Systems*, 22(3):2432–2458, 2023.
- [21] Gregory L Watson, Di Xiong, Lu Zhang, Joseph A Zoller, John Shamshoian, Phillip Sundin, Teresa Bufford, Anne W Rimoin, Marc A Suchard, and Christina M Ramirez. Pandemic velocity: Forecasting covid-19 in the us with a machine learning & bayesian time series compartmental model. *PLoS computational biology*, 17(3):e1008837, 2021.

- [22] Bakary Traore, Ousmane Koutou, and Boureima Sangare. A global mathematical model of malaria transmission dynamics with structured mosquito population and temperature variations. *Nonlinear Analysis: Real World Applications*, 53:103081, 2020.
- [23] Jacob C Koella. On the use of mathematical models of malaria transmission. *Acta tropica*, 49(1):1–25, 1991.
- [24] Nakul Chitnis, James M Hyman, and Jim M Cushing. Determining important parameters in the spread of malaria through the sensitivity analysis of a mathematical model. *Bulletin of mathematical biology*, 70:1272–1296, 2008.
- [25] Nakul Chitnis, Jim M Cushing, and JM Hyman. Bifurcation analysis of a mathematical model for malaria transmission. *SIAM Journal on Applied Mathematics*, 67(1):24–45, 2006.
- [26] Mojeeb Osman and Isaac Adu. Simple mathematical model for malaria transmission. *Journal of Advances in Mathematics and Computer Science*, 25(6):1–24, 2017.
- [27] Harry J Dudley, Abhishek Goenka, Cesar J Orellana, and Susan E Martonosi. Multi-year optimization of malaria intervention: a mathematical model. *Malaria journal*, 15:1–23, 2016.
- [28] Abadi Abay Gebremeskel and Harald Elias Krogstad. Mathematical modelling of endemic malaria transmission. *American Journal of Applied Mathematics*, 3(2):36–46, 2015.
- [29] Steffen E Eikenberry and Abba B Gumel. Mathematical modeling of climate change and malaria transmission dynamics: a historical review. *Journal of mathematical biology*, 77(4):857–933, 2018.